



Universiteit
Leiden
The Netherlands

Activity-based proteasome profiling

Li, N.

Citation

Li, N. (2016, December 16). *Activity-based proteasome profiling*. Retrieved from <https://hdl.handle.net/1887/22870>

Version: Not Applicable (or Unknown)

License: [Licence agreement concerning inclusion of doctoral thesis in the Institutional Repository of the University of Leiden](#)

Downloaded from: <https://hdl.handle.net/1887/22870>

Note: To cite this publication please use the final published version (if applicable).

Cover Page



Universiteit Leiden



The handle <http://hdl.handle.net/1887/22870> holds various files of this Leiden University dissertation

Author: Li, Nan

Title: Activity-based proteasome profiling

Issue Date: 2013-12-16

6

Activity-based protein profiling reveals reactivity of the murine thymoproteasome-specific subunit β_5t

Florea BI, Verdoes M, Li N, van der Linden WA, Geurink PP, van den Elst H, Hofmann T, de Ru A, van Veelen PA, Tanaka K, Sasaki K, Murata S, den Dulk H, Brouwer J, Ossendorp FA, Kisselev AF, Overkleeft HS, Chem Biol. 2010, 17, 795-801.

6.1 Introduction

The ability to recognise non-self oligopeptides is a key feature of mammalian immunity. T cells that recognise antigenic oligopeptides elicit a directed adaptive immune response aimed at the identification and eventual eradication of the invading pathogen that is the source of the non-self protein from which the antigenic oligopeptide is derived(1, 2). T cell recognition is effected by binding of specific T cell receptors to the antigenic peptides that are complexed to either major histocompatibility complex (MHC) class I or MHC class II molecules(3, 4). MHC I molecules present oligopeptides derived from cytosolic and nuclear proteins to CD8+ cytotoxic T lymphocytes (CTL) and by this virtue report on the presence of virally encoded proteins(5). T cells specific for non-self peptides are produced by thymic selection. The generation in the thymus of non-self peptide selective CTL proceeds in two discreet events(6). Positive selection is mediated by cortical thymic epithelial cells. In this process, thymocytes expressing T cell receptors are confronted with tissues expressing MHC I molecules loaded with oligopeptides. Current understanding is that the peptide antigens produced by cortical thymic epithelial cells are low affinity MHC I binders. Thymocytes, passing through the thymic cortex, that bind to MHC I molecules carrying a peptide load are selected from thymocytes expressing non-binding receptors. In the ensuing negative selection step, mediated by medullary thymic epithelial cells, thymocytes from the positively selected pool that are responsive to MHC I molecules exposing self peptides are eliminated.

Recently, Tanaka and co-workers made a major breakthrough towards understanding how positive selection proceeds(7). They found that epithelial cells at the thymic cortex express, next to the constitutive proteasome and the immunoproteasome, a third 20S proteasome particle which was dubbed the thymoproteasome. The 20S core particle of the proteasome is assembled from α and β subunits in a pattern of four, stacked,

heptameric rings ($\alpha 1-7$, $\beta 1-7$, $\beta 1-7$, $\alpha 1-7$) generating a barrel-shaped structure that contains 2 copies of the catalytically active β -subunits: $\beta 1$ (post acidic), $\beta 2$ (tryptic-like), $\beta 5$ (chymotryptic-like) peptidase activities(8). The thymoproteasome contains the $\beta 1i$ and $\beta 2i$ subunits just like the immunoproteasome, with the important exception that the unique subunit $\beta 5t$ replaces the immunoproteasome specific subunit, $\beta 5i$.

The thymoproteasome is the most abundant proteasome species in cortical thymic epithelial cells (cTEC). Thymoproteasome expression may have implications for the repertoire of oligopeptides presented by MHC I molecules on the surface of cTEC's that might significantly differ from the repertoire produced by medullary thymic epithelial cells. Closer inspection of the thymoproteasome 20S particle revealed that, in contrast to the constitutive and the immunoproteasome, it possessed little chymotryptic activity, a finding that seems to correlate with the hydrophilic nature of the putative substrate-binding site of $\beta 5t$ compared to $\beta 5/\beta 5i$ (7). In theory $\beta 5t$ can contribute in two ways to the generation of specific MHC I peptides used in positive T cell selection(9). It could act as an impassive, catalytically inactive bystander, in which case $\beta 1i/\beta 2i$ produce the majority of MHC I peptides with a bias towards their substrate preferences. Alternatively, it could actively participate in protein degradation and assist in producing 'non-self' peptides thanks to its intrinsic substrate preference, which then must be distinct from that of $\beta 5/\beta 5i$.

Activity-based probes are synthetic compounds bearing a reporter or affinity tag and an enzyme reactive group that can covalently bind to the active site of an enzyme(10). The tagged enzymatic activities can then be visualized by fluorescence or affinity purified, digested with trypsin and identified by LC/MS analysis. This Chapter demonstrates, by making use of activity-based proteasome probes(11), that $\beta 5t$ is in fact a catalytically active subunit, and show that its preference towards established proteasome inhibitors differs substantially from those of $\beta 5/\beta 5i$.

6.2 Results and discussion

6.2.1 Activity-based profiling reveals $\beta 5t$ activity

As the first experiment, whole tissue thymus homogenate from 3 weeks old mice was incubated with the fluorescent broad-spectrum ABP's **1**, **2**, **4** and MV151 shown in Figure 1 (for the synthesis of probes **2** and **4** see supplemental methods) (12, 13). Proteins were resolved by SDS-PAGE under reducing conditions and fluorescently labeled proteasome subunits were visualized by in-gel fluorescence scanning. In Figure 2A, MV151 shows the typical band pattern of staining that is similar to that of the EL4 cell line expressing the constitutive and the immunoproteasome (see supplemental Figure S1) indicating that both particles are expressed in the thymus(14). Peptide vinyl sulphone **1**, the biotinylated derivative of MV151, shows a similar pattern as MV151. Interestingly, the peptide epoxyketones **2** and **4** show two new bands that run below and above the

constitutive and immunoproteasome subunits. Of these, the lower band corresponds to β_{1i} .

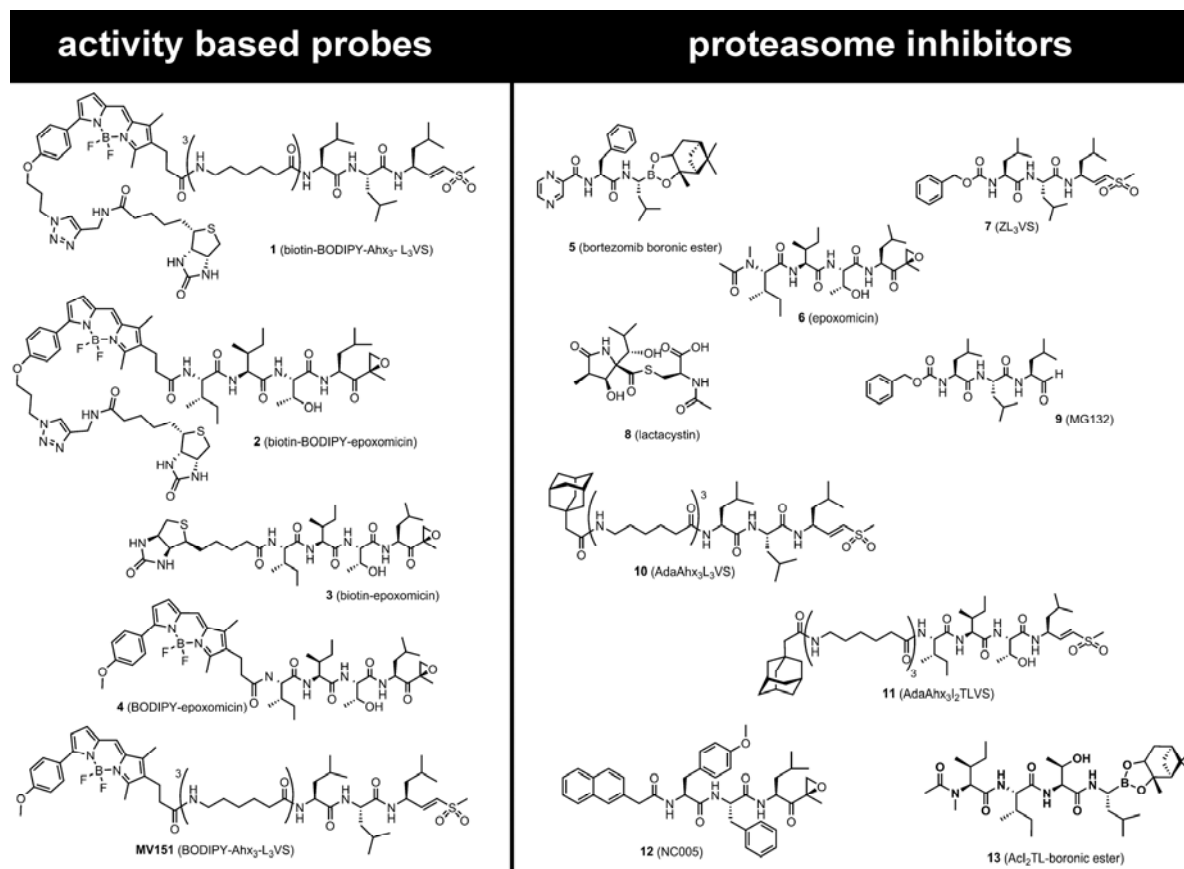


Figure 1: Activity-based probes and proteasome inhibitors used in this study.

In addition to the enzyme reactive group (warhead) and targeting sequence of the inhibitors, activity-based probes are equipped with a fluorophore for in-gel detection, a biotin tag for affinity purification or with both.

To ascertain whether the new, epoxyketone sensitive protein, with a gel mobility corresponding to the predicted molecular weight of $\beta_{5t}(7)$, is indeed β_{5t} and not a thymus-specific gene product unrelated to the thymoproteasome, a pull-down experiment was performed by making use of the biotin moiety present in ABPs **1** and **2**. Biotinylated proteins from thymus homogenate were captured by streptavidin-coated magnetic beads, resolved by SDS-PAGE and detected both by fluorescence and silver staining. Figure 2B shows the specific purification of several proteins that run in a pattern similar with that of Figure 2A. Protein ID, indicated by arrows in Figure 2B, was determined by on-bead (Table S1) and in-gel tryptic digestion followed by LC-MS/MS analysis. Oligopeptides corresponding to the expected constitutive proteasome ($\beta_1/\beta_2/\beta_5$) and immunoproteasome ($\beta_{1i}/\beta_{2i}/\beta_{5i}$) were captured by ABP **1** but no evidence for β_{5t} was

found. Peptides derived from β_{5t} were found by affinity purification with ABP **2**, indeed in the band running higher than the other active β subunits. However, the protein yield achieved by pull-down with ABP **1** and **2** was low. Then, the short biotinylated epoxomicin ABP **3** might increase the pull-down efficiency was synthesized to enhance the pull down efficiency (for the synthesis of probe **3** see supplemental methods). ABP **3** performed as expected, showing bands of similar pattern as ABP **2**, stronger signal in silver stained gels and reliable LC-MS identification of proteins that is presented in Table 1.

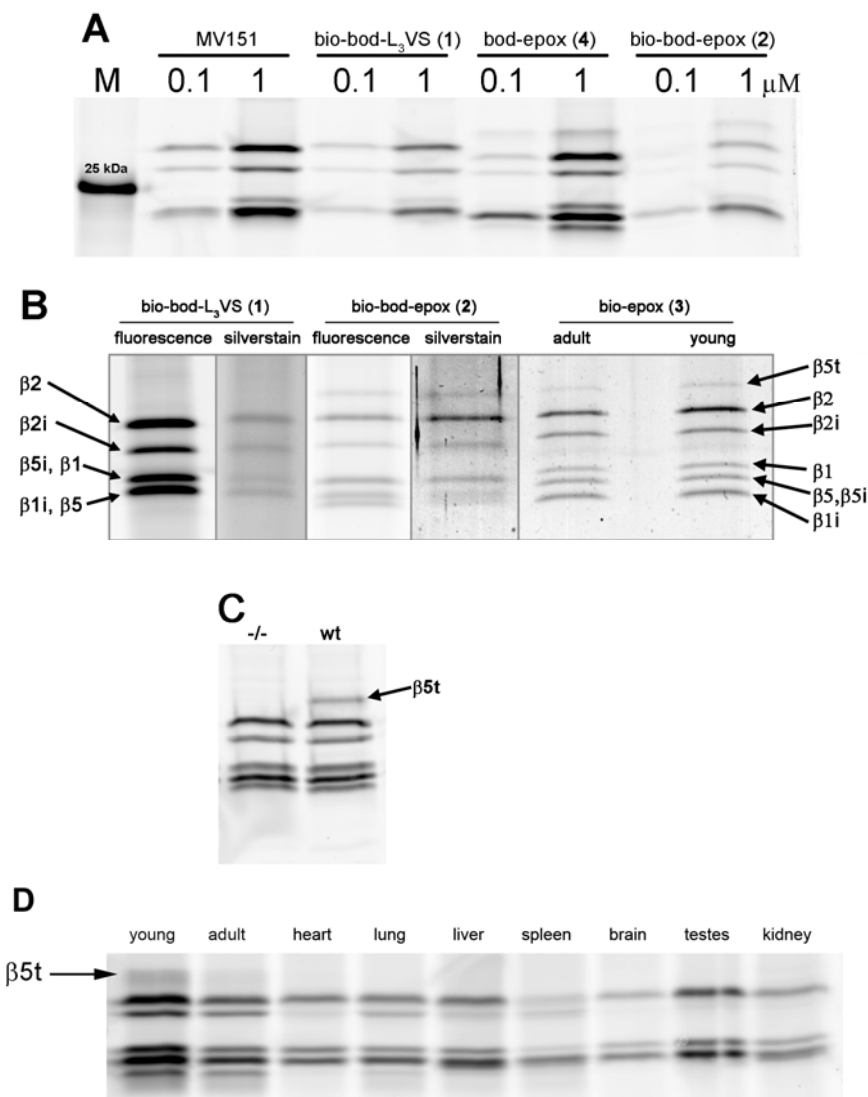


Figure 2: Activity-based protein profiling, affinity purification and LC-MS identification of proteasome β subunits in murine tissues lysates.

(A) In-gel fluorescence detection of active proteasome β subunits in 3 weeks old wild type murine thymus homogenate after labeling with MV151, ABP **1**, **2** and **4**.

(B) In-gel fluorescence and silver stain detection of active proteasome β subunits in young and adult thymus after labeling with ABP **1**, **2**, **3** and affinity purification. Protein

identification by LC-MS analysis of in-gel digested silver stained bands (indicated by arrows).

(C) In-gel fluorescence detection with ABP **4** of β 5t activity in wild type and absence of activity in the (-/-) β 5t knock down thymus from 3 weeks old mice.

(D) Activity-based proteasome profiling using ABP **4** shows β 5t activity in murine thymus (young and adult) but not in heart, lung, liver, spleen, brain, testes and kidney.

Table 1: Protein identification of silver stained bands captured by probe **3** in Figure 2B, by in-gel digestion and LC-MS analysis.

prot acc		mass	cover	pept			
		(Da)	% AA	z	ppm	score	peptide sequence
Psmb11	(β 5t)	27834	20	2	-0.29	50	SLEQELEAK
IPlo0221461				2	-0.54	39	ESGWEYVSR
				2	0.05	34	LLGTTSGTSADCATWYR
				3	0.00	25	GYHYDMTIQEAYTLAR
Psmb7	(β 2)	25235	57	2	-1.20	41	GTTAVLTEK
IPlo0136483				2	0.39	64	DGIVLGADTR
				3	0.14	42	FRPDMEEEEAK *
				2	-0.63	45	LDFLRPFVSPNK *
				3	0.58	34	LDFLRPFVSPNKK **
				2	2.14	130	LPYVTMGSGSLAAMAVFEDK
				3	-0.19	64	VTPLEIEVLEETVQTMDS #
				4	5.34	100	IHFISPNIYCCGAGTAADTDMTTQLISSNLELHSLTTGR
Psmb10	(β 2i)	24789	18	2	0.20	25	DGVILGADTR
IPlo0316736				2	-0.42	44	ALSTPTEPVQR
				2	1.54	85	EVRPLTLELLEETVQAMEVE #
Psmb6	(β 1)	21982	48	2	0.09	56	QVLLGDQIPK
IPlo0119239				2	-2.05	76	LAAIQESGVER
				2	-0.46	132	DECLQFTANALALAMER
				2	1.65	100	QSFAIGSGSSYIYGYVDATYR
				4	4.96	36	SGSAADTQAVADAVTYQLGFHSIELNEPPLVHTAASLFK

Psmb8	(β 5i)	22635	42	2	0.71	72	ATAGSYISLR
IPlo0116712				2	0.00	42	FQHGIVAVDSR
				2	-1.03	73	VESSDVSDLLYK
				2	-0.35	63	GPGLYYVDDNGTR
				2	-0.34	60	QDLSPEEAYDLGR
				2	0.95	72	VIEINPYLLGTMSGCAADCQYWER
Psmb5	(β 5)	22514	13	2	0.23	24	ATAGAYIASQTVK
IPlo0317902				2	-0.28	48	GPGLYYVDSSEGNR
Psmb9	(β 1i)	21313	17	2	0.67	79	FTTNAITLAMNR
IPlo0309379				2	-0.43	101	DGSSGGVIYLVITAAAGVDHR

Table 1. Protein name, mass of the active β subunit, % coverage of the protein by amino acids identified by LC-MS, charge of the peptide (z), measurement error (ppm), Mascot peptide scores, one (*) or two (**) miss cleavages, and C-terminal peptides (#). Mascot identifications were manually validated.

Thymus from adult animals treated in the same fashion shows β 5t activity as well, which suggests that the murine thymoproteasome remains active for at least 6 months. Next to the active proteasome β subunits, only four endogenously biotinylated background proteins were recovered with this method, a result that reflects the selectivity of ABPs **1**, **2**, **3**, and **4** towards proteasomes. Thymus lysates of 2 weeks old mice in which the β 5t protein expression was genetically knocked down show normal activity of immuno- and constitutive proteasome compared with the wild type, but complete absence of β 5t activity (Figure 2C). To characterize the expression of β 5t in murine tissues a tissue scan was performed with ABP probe **4**. Figure 2D shows that β 5t activity is exclusively present in the young thymus and at lower activity in thymus of 6 months old mice. Integration of the fluorescent signal from young thymus indicated that β 5t contributes to some 4% of the total active subunits signal in this full thymus lysate. Heart, lung, liver, spleen, brain, testes and kidney do not show β 5t activity. The presence of immunoproteasome bands in the heart, lung, liver and spleen tissues is explained by the presence of lymphocytes in these organs.

6.2.2 LC-MS³ analysis of the β 5t active-site peptide

Isolation and analysis of the active-site peptide covalently bound to ABP probe **3** would be the ultimate proof for the β 5t activity. Biotin-epoxomicin binds to the catalytic N-terminal threonine via an irreversible morpholino ring formation shown in Figure 3A. The β 5t active-site peptide (Figure 3B) is generated after denaturation and tryptic digest of the

thymoproteasome. Given that biotin-epoxomicin binds to all active β subunits, 6 different active-site peptides were expected because the tryptic peptides derived from β_5 and β_{5i} are identical (see Table S2). After LC-MS analysis, the active-site peptides were identified from the high resolution full MS scans by their exact mass and charge (Figure 3C). Further evidence was provided by the MS/MS (MS^2) fragmentation that revealed the presence of the biotin-epoxomicin signature ions b_1 , b_2 , b_3 , and b_4 from Figure 3D. In fact, the favored fragmentation of the morpholino ring, due to push-pull radical stabilization of the ions, yields mainly two major ions b_4 and y_7 where y_7 contains the peptide sequence of the β subunit active-site(15). By electrostatic trapping and further MS^3 fragmentation of the y_7 ion, the LAFR sequence of the β_{5t} active-site peptide was identified (Figure 3E). Taken together, this data set demonstrates that β_{5t} is, indeed, a catalytically active proteasome subunit.

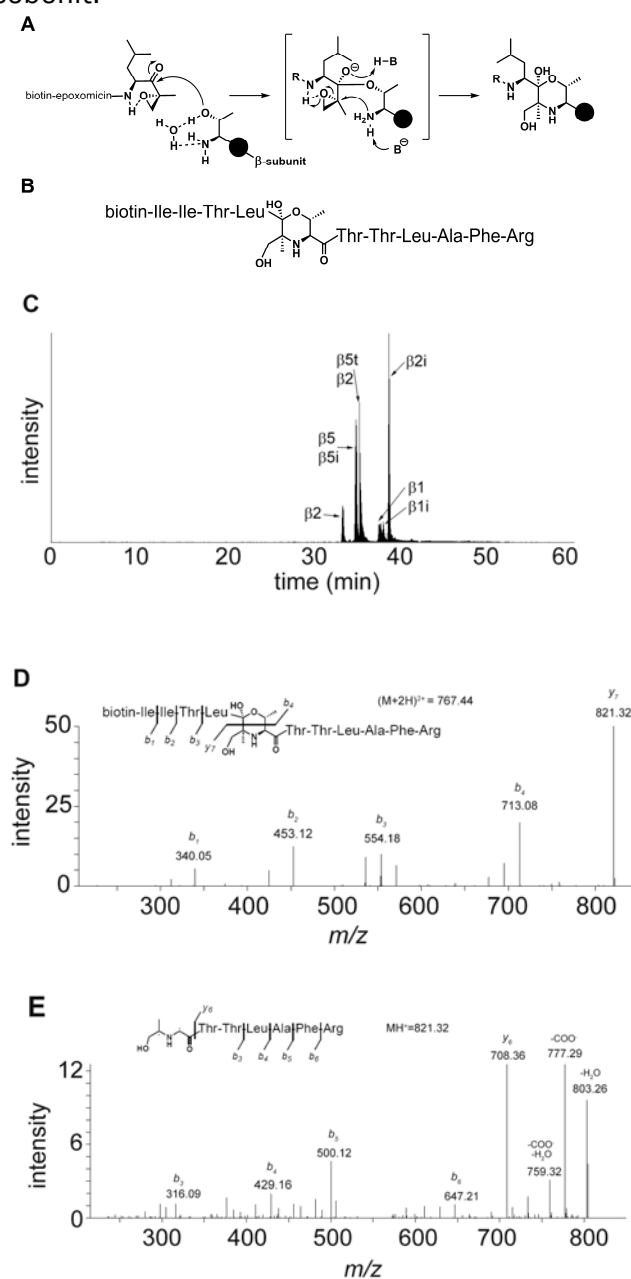


Figure 3: Active-Site Peptide Identification and Determination of Proteasome β subunits by Affinity Purification, Tryptic digest and LC-MS analysis.

(A) Reaction mechanism of biotin-epoxomicin **3** with the catalytically active N-terminal Thr residue of active proteasome β subunits. The morpholino ring formation results in a covalent and irreversible binding.

(B) Schematic representation of the biotin-epoxomicin modified, N-terminal active site tryptic peptide of β_{5t} . Amino acid residues are represented in a 3-letter code.

(C) LC-MS elution profile of the six unique biotinylated tryptic peptides derived from the active sites. Notice that β_5 and β_{5i} active site peptides are identical (see Table S2)

(D) LC- MS^2 determination of the β_{5t} active site fragmentation pattern. The parent ion (m/z ($M+2H$) $^{2+}$ = 767.44) was fragmented. The b_1 , b_2 , b_3 and b_4 ions are signature ions of the biotin-

epoxomicin N-terminal part. The abundant $\gamma 7$ ion containing the $\beta 5t$ active site peptide sequence was selected for further (MS^3) fragmentation (see panel (E)).

(E) LC- MS_3 determination of the $\gamma 7$ ion ($MH^+ = 821.32$) revealing the $\beta 5t$ active site peptide amino acid sequence.

6.2.3 Competitive activity-based protein profiling reveals $\beta 5t$ substrate specificity

The finding that $\beta 5t$ reacts with epoxyketones **2**, **3**, and **4** but not with peptide vinyl sulphones **1** and MV151, gives a first indication of an altered substrate specificity compared to $\beta 5/\beta 5i$. With probe **4** in hand as read-out, investigation was set out to reveal the $\beta 5t$ substrate preference by competitive activity-based studies with established proteasome inhibitors of diverse chemical characteristics.

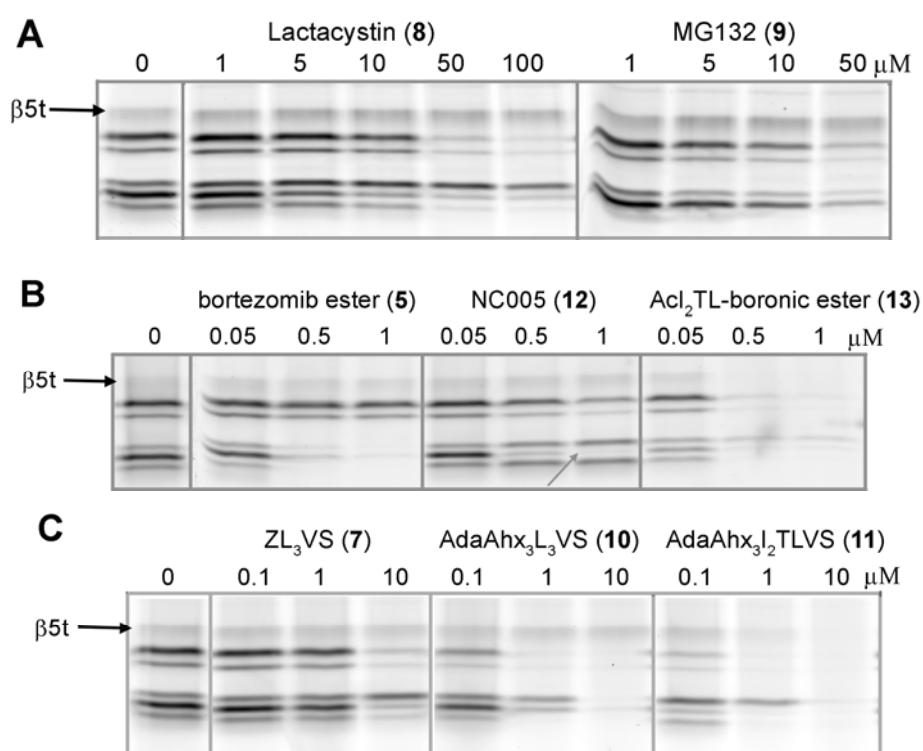


Figure 4: Analysis of $\beta 5t$ substrate specificity in Juvenile murine thymus lysates by competitive activity-based protein profiling with ABP **4**.

(A) Lysates were exposed to increasing concentrations Lactacystin or MG132, residual $\beta 5t$ activity was stained with ABP **4** and visualized by in-gel fluorescence detection. The inhibitors are not reactive towards the $\beta 5t$ activity.

(B) Bortezomib efficiently inhibits $\beta 5$, $\beta 5i$, $\beta 1$ and $\beta 1i$ activity but not $\beta 5t$. NC005 specifically targets $\beta 5$ (indicated by the grey arrow) but not $\beta 5t$. The mixed inhibitor containing the boronic ester warhead equipped with the epoxomicin tail efficiently blocks $\beta 5t$.

(C) In analogy to (B), installation of the epoxomicin IleLeuThrLeu peptide targeting motif to the vinyl sulphone warhead affords a potent inhibitor of the $\beta 5t$ activity.

Figure 4A shows the results of the most commonly used proteasome inhibitors lactacystin and MG132(16, 17). Both require concentrations higher than 10 μ M for broad-spectrum proteasome inhibition with marked affinity for β_5 and β_2 , but do not inhibit the β_{5t} activity. Figure 4B shows that the Bortezomib boronic ester **5** effectively blocks β_1 , β_{1i} , β_5 and β_{5i} as previously described(11, 18), while the subunit specific inhibitor NCo05 selectively inhibits the β_5/β_{5i} subunits(19), but neither interacts with the β_{5t} . However, mixing of the potent boronic ester warhead with the AcI2TL peptide sequence inherent to epoxomicin as in compound **13**, abolished the subunit preference of Bortezomib and efficiently inhibited β_{5t} . A similar effect is revealed in Figure 4C where the vinyl sulphone warhead was equipped with the AdaAhx3 extended I2TL motif. Apparently, the presence of the hydrophilic threonine side chain at P2 in an inhibitor or ABP probe is favorable for affinity to the β_{5t} subunit(20). From the results, some interesting trends pointing towards a substrate preference of β_{5t} that is rather distinct to that of β_5/β_{5i} appear. Whereas β_{5t} is sensitive towards the broad-spectrum proteasome epoxomicin **6**, it is quite unreactive towards the β_5/β_{5i} biased compounds. Bortezomib boronic ester **5** (which at the concentrations used disables $\beta_1/\beta_{1i}/\beta_5/\beta_{5i}$) and lactacystin **8** are inactive towards β_{5t} , as is the case with vinyl sulfone **7**, peptide aldehyde **9** and epoxyketone **12**. Altogether, our data, revealing that β_{5t} is catalytically active towards inhibitors more hydrophilic than those recognized by β_5/β_{5i} , point towards the involvement of β_{5t} in the generation of a unique set of oligopeptides complexed to MHC I molecules for optimal positive T cell selection.

6.3 Conclusion

In summary, it is proved for the first time that β_{5t} is catalytically active. Interestingly, active β_{5t} is also found in adult thymi. The first insight into the nature of the substrate preference of β_{5t} is also provided. This body of evidence was made possible by the direct action of activity-based probes with emphasis on the bi-functional ABPs that facilitate both read-out and affinity purification. A more thorough investigation is needed to establish the nature of substrates accepted by β_{5t} , and thus the nature of the MHC I peptides produced by the thymoproteasome in the positive T cell selection process.

6.4 Experimental procedure

6.4.1 Animals and tissues

Thymus and other organs were isolated from young (3 weeks) or adult mice and kindly provided by Ine Tijdens, Chantal Pont and Prof Dr. Bob van de Water. Thymus from β_{5t} knock-out mice was kindly provided by Dr Tanaka. Organ isolation was approved by the animal experimentation ethical committee of the Leiden University and Tokyo Metropolitan Institute of Medical Science.

6.4.2 Compounds

Design, synthesis and mechanism of action of the activity-based probes **1-4**, MV151 and the proteasome inhibitors **5-11**, **13** is reviewed in ((12) and the references therein). NCo05 is described in Britton et al.(19). Lactacystin, MG132 and all other compounds of analytical grade were purchased from Sigma-Aldrich.

Fmoc-Ile-Thr(tBu)-OMe

L-threonine(tBu) methyl ester HCl salt (2.5 g, 11 mmol) was dissolved in DCM (60 mL). To this solution were added Fmoc-L-isoleucine (4.7 g, 13.3 mmol, 1.2 equiv.), HCTU (5.5 g, 13.3 mmol, 1.2 equiv.) and DIPEA (6.0 mL, 36 mmol, 3.3 equiv.). The mixture was stirred for 2 hours after which TLC analysis indicated a completed reaction. The mixture was concentrated in vacuo, dissolved in EtOAc and extracted with 1 M HCl (2x), saturated NaHCO₃ (2x) and brine. The organic layer was dried (MgSO₄) and concentrated under reduced pressure. Purification of the product by column chromatography (10% → 15% EtOAc/petroleum ether) gave the title compound as a colorless solid (yield: 5.16 g, 9.83 mmol, 89%). ¹H NMR (400 MHz, CDCl₃) δ = 7.76 (d, J = 7.48 Hz, 2H), 7.60 (d, J = 7.41 Hz, 2H), 7.39 (t, J = 7.46, 7.46 Hz, 2H), 7.31 (dt, J = 7.43, 7.43, 0.98 Hz, 2H), 6.48 (d, J = 8.84 Hz, 1H), 5.58 (d, J = 8.70 Hz, 1H), 4.49 (dd, J = 9.00, 1.68 Hz, 1H), 4.44-4.33 (m, 2H), 4.28-4.15 (m, 3H), 3.71 (s, 3H), 1.94-1.83 (m, 1H), 1.65-1.53 (m, 1H), 1.33-1.21 (m, 1H), 1.17 (d, J = 6.27 Hz, 3H), 1.11 (s, 9H), 1.03-0.93 (m, 6H) ppm. ¹³C NMR (100 MHz, CDCl₃) δ = 171.426, 170.868, 156.074, 143.910, 143.784, 141.249, 127.635, 127.017, 125.077, 119.904, 74.215, 67.193, 66.969, 59.307, 57.832, 52.135, 47.173, 38.179, 28.272, 24.820, 21.046, 15.085, 11.521 ppm.

Boc-Ile-Ile-Thr(tBu)-NHNH₂

Fmoc-Ile-Thr(tBu)-OMe (5.16 g, 9.83 mmol) was dissolved in DMF (50 mL) and DBU (1.57 mL, 10.3 mmol, 1.05 equiv.) was added. The reaction was stirred for 5 minutes after which TLC analysis showed complete removal of the Fmoc group. Next, HOBt (1.98 g, 14.7 mmol, 1.5 equiv.) was added and the reaction mixture was stirred for another 30 minutes. To this mixture were added Boc-L-isoleucine (2.73 g, 11.8 mmol, 1.2 equiv.), HCTU (4.88 g, 11.8 mmol, 1.2 equiv.) and DIPEA (4.87 mL, 29.5 mmol, 3 equiv.). The mixture was stirred for 16 hours after which TLC analysis indicated a completed reaction. The mixture was concentrated in vacuo, dissolved in DCM and extracted with 1 M HCl (2x), saturated NaHCO₃ (2x) and brine. The organic layer was dried (MgSO₄) and concentrated under reduced pressure. Purification of the product by column chromatography (10% → 50% EtOAc/petroleum ether) gave Boc-Ile-Ile-Thr(tBu)-OMe as a colorless solid (yield: 3.69 g, 7.15 mmol, 73%). LC-MS: gradient 10% → 90% ACN/(0.1% TFA/H₂O): Rt (min): 9.88 (ESI-MS (m/z): 516.13 (M + H⁺)). The obtained product was dissolved in MeOH (50 mL) and hydrazine hydrate (10.4 mL, 214.5 mmol, 30 equiv.) was added. The reaction mixture was refluxed for 16 hours after which TLC analysis indicated complete conversion. Toluene was added and the mixture was concentrated under reduced pressure. Traces of hydrazine were

removed by co-evaporating the mixture with toluene (3x) and the title compound was obtained as a colorless solid (yield: 6.67 g, 7.15 mmol, quant.). ^1H NMR (400 MHz, MeOD) δ = 4.36 (d, J = 3.53 Hz, 1H), 4.32 (d, J = 8.12 Hz, 1H), 4.07-4.00 (m, 1H), 3.94 (d, J = 7.90 Hz, 1H), 1.93-1.84 (m, 1H), 1.83-1.73 (m, 1H), 1.61-1.50 (m, 2H), 1.44 (s, 9H), 1.19 (s, 9H), 1.19-1.16 (m, 2H), 1.10 (d, J = 6.32 Hz, 3H), 0.94-0.87 (m, 12H) ppm. ^{13}C NMR (100 MHz, MeOD) δ = 174.839, 173.393, 171.301, 157.910, 80.568, 75.849, 68.522, 60.624, 59.227, 58.566, 37.949, 37.852, 28.772, 28.668, 25.941, 19.781, 16.231, 15.951, 11.392, 11.325 ppm. LC-MS: gradient 10% \rightarrow 90% ACN/(0.1% TFA/H₂O): R_t (min): 6.08 (ESI-MS (m/z): 516.4 ($M + H^+$)).

Boc-Ile-Ile-Thr(tBu)-leucinyl-(R)-2-methyloxirane

Boc-Ile-Ile-Thr(tBu)-NHNH₂ (2.0 g, 3.87 mmol) was dissolved in DCM (40 mL) and cooled to -30°C under an argon atmosphere. tBuONO (566 μL , 4.25 mmol, 1.1 equiv.) and HCl (2.8 equiv., 10.8 mmol, 2.7 mL of a 4 M solution in 1,4-dioxane) were added and the mixture was stirred at -30 °C for 3 hours. (Boc-leucinyl)-(R)-2-methyloxirane (1.16 g, 4.25 mmol, 1.1 equiv.) was deprotected with DCM/TFA (1:1 v/v, 20 mL) for 30 minutes followed by co-evaporation with toluene (3x). The resulting TFA salt was dissolved in DMF (5 mL) and added to the former reaction mixture together with DiPEA (3.31 mL, 20 mmol, 5 equiv.). The reaction mixture was slowly warmed to ambient temperature and stirred for 16 hours. Next, the mixture was extracted with 1 M HCl (2x), H₂O and brine, dried (MgSO₄) and concentrated in vacuo. The title compound was obtained after column chromatography (20% \rightarrow 50% EtOAc/petroleum ether) as a colorless solid (yield: 2.25 g, 3.43 mmol, 89%). ^1H NMR (400 MHz, CDCl₃) δ = 7.64 (d, J = 7.47 Hz, 1H), 6.99 (d, J = 5.64 Hz, 1H), 6.45 (d, J = 8.20 Hz, 1H), 5.22 (d, J = 7.85 Hz, 1H), 4.46 (ddd, J = 10.45, 7.55, 2.94 Hz, 1H), 4.40-4.32 (m, 2H), 4.14-4.07 (m, 1H), 3.94 (t, J = 7.34, 7.34 Hz, 1H), 3.38 (d, J = 5.07 Hz, 1H), 2.89 (d, J = 5.06 Hz, 1H), 1.93-1.77 (m, 2H), 1.74-1.64 (m, 1H), 1.60-1.55 (m, 1H), 1.52 (s, 3H), 1.51-1.46 (m, 2H), 1.44 (s, 9H), 1.28 (s, 9H), 1.27-1.24 (m, 1H), 1.17-1.08 (m, 2H), 1.06 (d, J = 6.44 Hz, 3H), 0.96 (d, J = 6.54 Hz, 6H), 0.92-0.86 (m, 12H) ppm. ^{13}C NMR (100 MHz, CDCl₃) δ = 208.062, 171.593, 170.738, 169.515, 155.807, 79.761, 75.492, 66.143, 59.249, 57.686, 56.956, 52.395, 50.746, 39.809, 37.300, 36.971, 28.280, 28.082, 25.423, 24.879, 24.695, 23.358, 21.359, 16.754, 15.532, 15.405, 11.285 ppm. LC-MS: gradient 10% \rightarrow 90% ACN/(0.1% TFA/H₂O): R_t (min): 11.31 (ESI-MS (m/z): 655.27 ($M + H^+$)).

Biotin-epoxomicin (3)

Boc-Ile-Ile-Thr(tBu)-leucinyl-(R)-2-methyloxirane (13.2 mg, 20.2 μmol) was dissolved in 2 mL DCM. TFA (2 mL) was added and the mixture was stirred for 20 min. The reaction mixture was co-evaporated with toluene (3x). The residue was dissolved in 1 mL DMF. Biotin-OSu (7 mg, 21 μmol , 1.01 equiv.) and DiPEA (8.3 μL , 50 μmol , 2.5 equiv.) were added and the mixture was stirred for 2 hr. The volatiles were removed in vacuo and the title compound was obtained after HPLC purification (yield: 5 mg, 6.9 μmol , 34%). ^1H NMR (400 MHz, MeOD) δ = 4.55 (dd, J = 10.63, 3.03 Hz, 1H), 4.48 (dd, J = 7.72, 4.85 Hz, 1H), 4.32-

4.20 (m, 4H), 4.06-3.99 (m, 2H), 3.25 (d, $J = 5.07$ Hz, 1H), 3.23-3.16 (m, 1H), 2.95-2.89 (m, 2H), 2.69 (d, $J = 12.71$ Hz, 1H), 2.33-2.20 (m, 2H), 1.90-1.77 (m, 2H), 1.78-1.30 (m, 13H), 1.24-1.11 (m, 5H), 0.95-0.86 (m, 18H) ppm. LC-MS: gradient 10% \rightarrow 90% ACN/(0.1% TFA/H₂O): R_t (min): 6.30 (ESI-MS (m/z): 725.7 ($M + H^+$)).

Azido-BODIPY-epoxomicin

Boc-Ile-Ile-Thr(tBu)-leucinyI-(R)-2-methyloxirane (7.9 mg, 12 μ mol) was dissolved in TFA (1 mL) and stirred for 30 min., before being coevaporated with toluene (3). The residue was dissolved in DMF (2 mL) and azido-BODIPY-OSu (6.6 mg, 12 μ mol, 1 equiv.) and DiPEA (8 μ L, 48 μ mol, 4 equiv.) were added and the reaction mixture was stirred for 12 hr. Concentration in vacuo, followed by purification by column chromatography (DCM \rightarrow 2% MeOH/DCM) yielded the title compound as a brown/red solid (yield: 5.4 mg, 5.7 μ mol, 47%). ¹H NMR (600 MHz, MeOD) δ = 7.88 (d, $J = 8.7$ Hz, 2H), 7.41 (s, 1H), 7.06 (d, $J = 3.9$ Hz, 1H), 6.99 (d, $J = 8.7$ Hz, 2H), 6.60 (d, $J = 3.9$ Hz, 1H), 4.55 (dd, $J_1 = 10.7$, $J_2 = 2.8$ Hz, 1H), 4.30 (d, $J = 5.0$ Hz, 1H), 4.22 (d, $J = 7.8$ Hz, 1H), 4.15-4.12 (m, 3H), 4.02 (p, $J = 6.1$ Hz, 1H), 3.54 (t, $J = 6.7$ Hz, 2H), 3.25 (d, $J = 5.1$ Hz, 1H), 2.92 (d, $J = 5.1$ Hz, 1H), 2.81 (m, 1H), 2.71 (m, 1H), 2.51 (s, 3H), 2.45-2.40 (m, 2H), 2.25 (s, 3H), 2.07 (p, $J = 6.3$ Hz, 2H), 1.89-1.79 (m, 1H), 1.75-1.66 (m, 2H), 1.65-1.52 (m, 2H), 1.53-1.41 (m, 5H), 1.41-1.21 (m, 15H), 1.20-1.06 (m, 5H), 1.05-0.97 (m, 1H), 0.97-0.85 (m, 16H), 0.82 (d, $J = 6.7$ Hz, 3H), 0.76 (t, $J = 7.4$ Hz, 3H) ppm. ¹³C NMR (150 MHz, MeOD) δ = 209.51, 174.86, 174.06, 173.59, 172.23, 161.03, 160.67, 156.57, 141.79, 136.67, 135.83, 132.45, 131.92, 131.89, 131.86, 131.67, 131.65, 129.91, 129.28, 127.16, 124.70, 119.10, 115.27, 115.19, 69.14, 68.55, 65.98, 60.13, 59.82, 59.42, 59.41, 53.10, 51.84, 40.38, 38.02, 37.71, 36.45, 30.82, 29.90, 26.26, 26.03, 23.81, 21.52, 21.21, 20.02, 17.05, 15.92, 15.86, 11.47, 11.22, 9.67 ppm.

Biotin-BODIPY(Tmr)-epoxomicin (2)

Azido-BODIPY(Tmr)-epoxomicin (4.1 mg, 4.3 μ mol) and Biotin-propargylamide (2.4 mg, 8.6 μ mol, 2 equiv.) were dissolved in tBuOH (0.25 mL) and toluene (0.25 mL) before CuSO₄ (125 μ L 3.4 mM, 10 mol%) and sodium ascorbate (125 μ L 6.9 mM, 20 mol%) were added. The reaction mixture was stirred at 80 °C for 12 hr., before being cooled to room temperature and concentrated in vacuo. Purification by column chromatography (petroleum ether \rightarrow 50% acetone/petroleum ether) yielded the title compound as a brown/red solid (4.5 mg, 3.7 μ mol, 85%). ¹H NMR (600 MHz, MeOD) δ = 7.95-7.78 (m, 3H), 7.42 (s, 1H), 7.07 (d, $J = 4.1$ Hz, 1H), 6.95 (d, $J = 8.9$ Hz, 2H), 6.61 (d, $J = 4.1$ Hz, 1H), 4.70-4.52 (m, 5H), 4.46-4.39 (m, 2H), 4.34-4.26 (m, 1H), 4.25-4.19 (m, 1H), 4.17-4.11 (m, 1H), 4.08-3.99 (m, 3H), 3.95 (t, $J = 2.2$ Hz, 1H), 3.25 (d, $J = 5.0$ Hz, 1H), 3.16-3.10 (m, 1H), 2.92 (d, $J = 5.1$ Hz, 1H), 2.71-2.64 (m, 2H), 2.60-2.56 (m, 1H), 2.51 (s, 3H), 2.46-2.37 (m, 4H), 2.26 (s, 3H), 2.24-2.17 (m, 2H), 1.95-1.21 (m, 32H), 1.21-1.10 (m, 5H), 1.06-0.85 (m, 17H), 0.82 (d, $J = 6.8$ Hz, 3H), 0.76 (t, $J = 7.3$ Hz, 3H) ppm.

6.4.3 Activity-based protein profiling

Tissues were homogenized in 3 volumes of ice cold lysis buffer (50 mM TrisHCl pH 7.5, 250 mM sucrose, 5mM MgCl₂, 1mM DTT, 2mM ATP, 0.025% digitonin, 0.2% NP₄₀, (21)) with a tissue homogenizer and further disrupted by 2 x 30 sec sonication. Lysates were cleared by cold centrifugation at 13,000 g, protein concentrations determined by Bradford assay and kept at -80°C until use. For comparative activity based profiling, equal amounts of protein were incubated with ABPs for 1 hr at 37°C, resolved by 12.5% SDS-PAGE and the wet gel slab was scanned on a Thyphoon scanner (GE Healthcare) with the TAMRA settings (λ_{ex} =530 nm, λ_{em} =560 nm). Competitive activity based profiling was done by first incubating thymus lysates with increasing concentrations of various proteasome inhibitors for 1 hr at 37°C, followed by 1 hr incubation with 0.5 μ M ABP **4** for the in-gel detection of the residual proteasome activity. Images were acquired, processed and quantified with Image Quant (GE Healthcare).

6.4.4 Affinity purification

Some 1 or 2 mg of protein was incubated with 10 μ M biotinylated ABPs **1**, **2** or **3** for 1 hr at 37°C, denatured by boiling for 5 min with 1% SDS and precipitated with chloroform/methanol (C/M, (22)). The protein pellet was rehydrated in 180 μ l 8M urea/100 mM NH₄HCO₃, reduced with 10 μ l 90 mM DTT for 30 min at 37°C, alkylated with 15 μ l 200 mM iodoacetamide at RT in the dark, cleared by centrifugation at 13,000 g and desalted by C/M. The pellet was dispersed in 25 μ l PD buffer (50 mM TrisHCl pH7.5, 150 mM NaCl) with 2% SDS in a heated (37°C) sonic bath. Stepwise (3 x 25 μ l, 4 x 100 μ l, 1 x 500 μ l) addition of PD buffer afforded a clear solution that was incubated with 50 μ l MyOne T1 Streptavidin grafted beads (Invitrogen) at RT with vigorous shaking for 2 hr. The beads were stringently washed with 2 x 300 μ l PD buffer with 0.1% SDS, 2 x 300 μ l PD buffer, 2 x 300 μ l wash buffer I (4M urea/50 mM NH₄HCO₃), 2 x 300 μ l wash buffer II (50 mM TrisHCl pH7.5, 10 mM NaCl) and 2 x 300 μ l water. For in-gel analysis, 2/3 of the beads was eluted with 100 μ l 1x sample buffer containing 10 μ M biotin by boiling for 5 min at 90°C and resolved by 12.5% SDS-PAGE. Proteins were visualized by fluorescence and silverstain, in-gel digested and desalted (23, 24). For on/bead digest, 1/3 of the beads was digested with 300 ng trypsin in 100 μ l digest buffer (100 mM TrisHCl pH 7.8, 100 mM NaCl, 1mM CaCl₂, 2% ACN) o.n. at 37°C. Peptides were collected and desalted on stage tips. The active-site peptides were eluted with 2 x 80 μ l 10 μ M biotin in 5% formic acid/25% ACN/70% H₂O for 30 min at 37°C and desalted after ACN evaporation.

6.4.5 LC-MS analysis

Tryptic peptides were analyzed on a Surveyor nanoLC system (Thermo) hyphenated to a LTQ-Orbitrap mass spectrometer (Thermo). Gold and carbon coated emitters

(OD/ID=360/25 μ m tip ID=5 μ m), trap column (OD/ID=360/100 μ m packed with 25 mm robust Poros®10R2/ 15 mm BioSphere C18 5 μ m 120Å) and analytical columns (OD/ID=360/75 μ m packed with 20 cm BioSphere C18 5 μ m 120Å) were from Nanoseparations (Nieuwkoop, The Netherlands). The mobile phases (A: 0.1% FA/H₂O, B: 0.1%FA/ACN) were made with ULC/MS grade solvents (Biosolve). The emitter tip was coupled end-to-end with the analytical column via a 15 mm long TFE teflon tubing sleeve (OD/ID 0.3x1.58 mm, Supelco, USA) and installed in a stainless steel holder mounted in a nano-source base (Upchurch scientific, Idex, USA).

General mass spectrometric conditions were: an electrospray voltage of 1.8 kV was applied to the emitter, no sheath and auxiliary gas flow, ion transfer tube temperature 150°C, capillary voltage 41V, tube lens voltage 150V. Internal mass calibration was performed with air-borne protonated polydimethylcyclsiloxane (m/z = 445.12002) and the plasticizer protonated dioctyl phthalate ions (m/z = 391.28429) as lock mass(25).

For shotgun proteomics analysis, 10 μ l of the samples was pressure loaded on the trap column with a 10 μ l/min flow for 5 min followed by peptide separation with a gradient of 35 min 5-30% B, 15 min 30-60% B, 5 min A at a flow of 300 μ l/min split to 250 nl/min by the LTQ divert valve. For each data dependent cycle, one full MS scan (300-2000 m/z) acquired at high mass resolution (60,000 at 400 m/z , AGC target 1×10^6 , maximum injection time 1,000 ms) in the Orbitrap was followed by 3 MS/MS fragmentations in the LTQ linear ion trap (AGC target 5×10^3 , max inj time 120 ms) from the three most abundant ions(26). MS² settings were: collision gas pressure 1.3 mT, normalized collision energy 35%, ion selection threshold of 500 counts, activation $q = 0.25$ and activation time of 30 ms. Fragmented precursor ions that were measured twice within 10 s were dynamically excluded for 60s and ions with $z < 2$ or unassigned were not analyzed.

A parent ion list of the m/z ratios of the active-site peptides was compiled and used for LC-MS³ analysis in a data dependent protocol. The parent ion was electrostatically isolated in the ion trap of the LTQ, fragmented by MS² and the most intense peak was isolated and further fragemented in MS³ to reveal the amino acid sequence of the active-site peptide. Data from MS² and MS³ was validated manually.

References and notes

1. Janeway, C. A., Jr., and Bottomly, K. (1994) Signals and signs for lymphocyte responses, *Cell* 76, 275-285.
2. Medzhitov, R. (2007) Recognition of microorganisms and activation of the immune response, *Nature* 449, 819-826.
3. Huseby, E. S., White, J., Crawford, F., Vass, T., Becker, D., Pinilla, C., Marrack, P., and Kappler, J. W. (2005) How the T cell repertoire becomes peptide and MHC specific, *Cell* 122, 247-260.

4. Takahama, Y., Tanaka, K., and Murata, S. (2008) Modest cortex and promiscuous medulla for thymic repertoire formation, *Trends Immunol* 29, 251-255.
5. Kloetzel, P. M., and Ossendorp, F. (2004) Proteasome and peptidase function in MHC-class-I-mediated antigen presentation, *Curr Opin Immunol* 16, 76-81.
6. Nitta, T., Murata, S., Ueno, T., Tanaka, K., and Takahama, Y. (2008) Thymic microenvironments for T-cell repertoire formation, *Adv Immunol* 99, 59-94.
7. Murata, S., Sasaki, K., Kishimoto, T., Niwa, S., Hayashi, H., Takahama, Y., and Tanaka, K. (2007) Regulation of CD8+ T cell development by thymus-specific proteasomes, *Science* 316, 1349-1353.
8. Baumeister, W., Walz, J., Zuhl, F., and Seemuller, E. (1998) The proteasome: paradigm of a self-compartmentalizing protease, *Cell* 92, 367-380.
9. Murata, S., Takahama, Y., and Tanaka, K. (2008) Thymoproteasome: probable role in generating positively selecting peptides, *Curr Opin Immunol* 20, 192-196.
10. Cravatt, B. F., Wright, A. T., and Kozarich, J. W. (2008) Activity-based protein profiling: from enzyme chemistry to proteomic chemistry, *Annu Rev Biochem* 77, 383-414.
11. Verdoes, M., Florea, B. I., van der Linden, W. A., Renou, D., van den Nieuwendijk, A. M., van der Marel, G. A., and Overkleeft, H. S. (2007) Mixing of peptides and electrophilic traps gives rise to potent, broad-spectrum proteasome inhibitors, *Org Biomol Chem* 5, 1416-1426.
12. Verdoes, M., Florea, B. I., van der Marel, G. A., and Overkleeft, H. S. (2009) Chemical Tools To Study the Proteasome, *Eur J Org Chem*, 3301-3313.
13. Verdoes, M., Florea, B. I., Menendez-Benito, V., Maynard, C. J., Witte, M. D., van der Linden, W. A., van den Nieuwendijk, A. M., Hofmann, T., Berkers, C. R., van Leeuwen, F. W., Groothuis, T. A., Leeuwenburgh, M. A., Ovaa, H., Neefjes, J. J., Filippov, D. V., van der Marel, G. A., Dantuma, N. P., and Overkleeft, H. S. (2006) A fluorescent broad-spectrum proteasome inhibitor for labeling proteasomes in vitro and in vivo, *Chem Biol* 13, 1217-1226.
14. Kessler, B. M., Tortorella, D., Altun, M., Kisselev, A. F., Fiebigler, E., Hekking, B. G., Ploegh, H. L., and Overkleeft, H. S. (2001) Extended peptide-based inhibitors efficiently target the proteasome and reveal overlapping specificities of the catalytic beta-subunits, *Chem Biol* 8, 913-929.
15. Carey, F. A., and Sundberg, R. J. (2007) *Advanced organic chemistry*, 5th ed., Springer, New York.
16. Fenteany, G., Standaert, R. F., Lane, W. S., Choi, S., Corey, E. J., and Schreiber, S. L. (1995) Inhibition of proteasome activities and subunit-specific amino-terminal threonine modification by lactacystin, *Science* 268, 726-731.
17. Rock, K. L., and Goldberg, A. L. (1999) Degradation of cell proteins and the generation of MHC class I-presented peptides, *Annu Rev Immunol* 17, 739-779.
18. Adams, J., Behnke, M., Chen, S., Cruickshank, A. A., Dick, L. R., Grenier, L., Klunder, J. M., Ma, Y. T., Plamondon, L., and Stein, R. L. (1998) Potent and selective inhibitors of the proteasome: dipeptidyl boronic acids, *Bioorg Med Chem Lett* 8, 333-338.

19. Britton, M., Lucas, M. M., Downey, S. L., Screen, M., Pletnev, A. A., Verdoes, M., Tokhunts, R. A., Amir, O., Goddard, A. L., Pelphrey, P. M., Wright, D. L., Overkleeft, H. S., and Kisselev, A. F. (2009) Selective inhibitor of proteasome's caspase-like sites sensitizes cells to specific inhibition of chymotrypsin-like sites, *Chem Biol* 16, 1278-1289.
20. Bogyo, M., McMaster, J. S., Gaczynska, M., Tortorella, D., Goldberg, A. L., and Ploegh, H. (1997) Covalent modification of the active site threonine of proteasomal beta subunits and the Escherichia coli homolog HslV by a new class of inhibitors, *Proc Natl Acad Sci U S A* 94, 6629-6634.
21. Kisselev, A. F., and Goldberg, A. L. (2005) Monitoring activity and inhibition of 26S proteasomes with fluorogenic peptide substrates, *Methods Enzymol* 398, 364-378.
22. Wessel, D., and Flugge, U. I. (1984) A method for the quantitative recovery of protein in dilute solution in the presence of detergents and lipids, *Anal Biochem* 138, 141-143.
23. Shevchenko, A., Tomas, H., Havlis, J., Olsen, J. V., and Mann, M. (2006) In-gel digestion for mass spectrometric characterization of proteins and proteomes, *Nat Protoc* 1, 2856-2860.
24. Rappsilber, J., Mann, M., and Ishihama, Y. (2007) Protocol for micro-purification, enrichment, pre-fractionation and storage of peptides for proteomics using StageTips, *Nat Protoc* 2, 1896-1906.
25. Olsen, J. V., de Godoy, L. M., Li, G., Macek, B., Mortensen, P., Pesch, R., Makarov, A., Lange, O., Horning, S., and Mann, M. (2005) Parts per million mass accuracy on an Orbitrap mass spectrometer via lock mass injection into a C-trap, *Mol Cell Proteomics* 4, 2010-2021.
26. Baek, D., Villen, J., Shin, C., Camargo, F. D., Gygi, S. P., and Bartel, D. P. (2008) The impact of microRNAs on protein output, *Nature* 455, 64-71.

Supplementary data

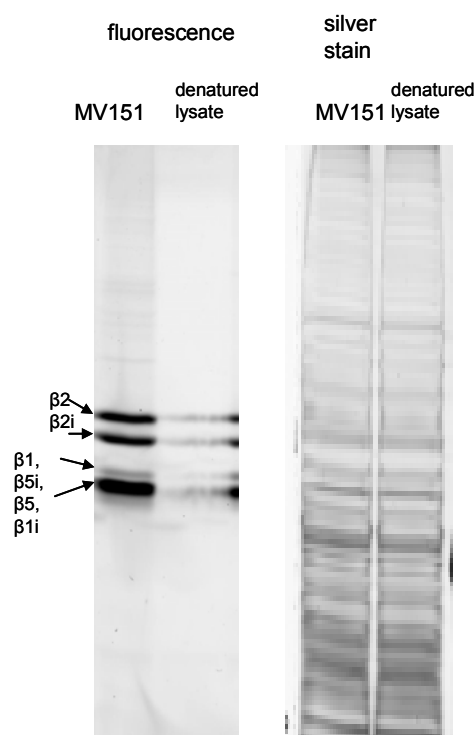


Figure S1. Fluorescence and silver stain detection of EL4 (murine B cell lymphoma cell line) cell lysate incubated with the fluorescent, broad-spectrum proteasome activity-based probe MV151. Some 20 μ g protein was incubated with 0.5 μ M MV151 for 60 min at 37°C, resolved by 12.5% SDS-PAGE and imaged by fluorescence scanning followed by silver staining of the same gel. In the denatured lane, the lysate was deactivated by boiling with 1% SDS prior to the MV151 incubation.

prot acc		mass (Da)	cover % AA	pept			peptide sequence
				z	ppm	score	
Psmb11	(β 5t)	27834	34	2	-0.89	47	HGVIAAADTR
IPI00221461				2	1.30	21	EGQLPSVAGTAK
				2	0.41	76	LLAAMMSCYR
				2	-2.14	93	SSCGSYVACPASR
				2	0.76	71	ACGIYPEPATPQGAR
				2	1.67	130	LLGTTSGTSADCATWYR
				2	1.89	99	ELFVEQEEVTPEDCAIIMK
Psmb7	(β 2)	25235	50	2	0.43	27	QMLFR
IPI00136483				2	1.09	70	FRPDMEEEEAK
				2	3.42	55	LDFLRPFSVPNK

				2	-0.80	57	FRPDMEEEEAKK *
				3	0.13	45	LDFLRPFSVPNKK *
				3	2.19	38	SKLDFLRPFSPVFNK *
				2	-4.89	62	LPYVTMGSGSLAAMAVFEDK
				2	-1.17	111	VTPLEIEVLEETVQTMDS #
				2	-0.11	129	LVSEAIAAGIFNDLGSGSNIDLCVSK
				3	3.18	57	KLVSEAIAAGIFNDLGSGSNIDLCVSK *
				3	0.28	173	IHFISPNYCCGAGTAADTDMTTQLISSNLELHSLTTGR
Psmb10	(β2i)	24789	65	2	-0.29	61	ATNDSVVADK
IPI00316736				2	0.00	40	MELHALSTGR
				2	-0.60	39	FAPGTTPLVLR
				2	-1.12	121	IYCCGAGVAADTEMTR
				2	0.35	167	LPFTALGSGQGAVALLEDK
				2	0.73	93	EVRPLTLELLEETVQAMEVE #
				4	0.77	53	YQGHV GASLVVGGVDLNGPQLYEVHPHGSYSR
Psmb6	(β1)	21982	74	2	0.35	58	DGSSGGVIR
IPI00119239				2	-0.21	50	FTIATLPPP #
				2	0.55	78	TTTGSYIANR
				2	1.28	91	LAAIQESGVER
				2	-1.59	55	LTPIHDHIFCCR
				2	1.59	132	DECLQFTANALALAMER
				2	1.27	129	QSFAIGSGSSYIYGYVDATYR
				3	1.68	32	EGMTKDECLQFTANALALAMER *
				3	1.68	106	YREDLMAGIIAGWDPQEGGQVYSPMGGMMVR *
				3	4.81	149	SGSAADTQAVADAVTYQLGFHSIELNEPPLVHTAASLFK
Psmb8	(β5i)	22635	55	2	-0.27	92	ATAGSYISLR
IPI00116712				2	2.60	66	LLSNMMLQYR
				2	-0.68	72	FQHGIVAVDSR
				2	-0.74	84	VESSDVSDLLYK
				2	0.56	80	GPGLYYVDDNGTR
				2	1.18	75	DNYSGGVVNMYHMK
				2	1.35	99	GMGLSMGSMICGWDK
				2	-0.75	121	LSGQMFSTGSGNTYAYGVMDSGYR

				3	0.81	60	VIEINPYLLGTMSGCAADCQYWER
Psmb5	(β5)	22514	18	2	0.38	47	VEEAYDLAR
IPI00317902				2	0.91	56	GPGLYYVDSEGNR
Psmb9	(β1i)	21313	58	2	0.21	56	VSAGTAVVNR
IPI00309379				2	-0.71	61	VILGDELPK
				2	-0.07	91	FTTNAITLAMNR
				2	0.05	96	DGSSGGVIYLVITITAAGVDHR
				3	-0.15	99	QPFTIGSGSGSSYIYGYVDAAYKPGMTPEECR
				3	-1.11	122	IFCALSGSAADAQAADMAAYQLELHGLEEPLVLAAANVVK

Table S1. Protein identification after affinity purification with probe **3**, on-bead digestion with trypsin and LC-MS analysis.

Protein name, mass of the active β subunit, % coverage of the protein by amino acids identified by LC-MS, charge of the peptide (z), measurement error (ppm), Mascot peptide scores, miss cleavage (*), and C-terminal peptides (#). Mascot identifications were manually validated.

	y_7 ion sequence	Exact mass		$z=2$		$z=3$	
		mono-iso	High-peak	mono-iso	High-peak	mono-iso	High-peak
$\beta 1$	TTIMAVQFNNGGVVLGADSR	2659.40773	2660.41061	1330.71114	1331.21258	887.47652	887.81081
$\beta 1i$	TTIMAVEFDGGVVVGSDSR	2663.35502	2664.35793	1332.68479	1333.18624	888.79228	889.12659
$\beta 2$	TTIAGVVYK	1674.96302	1674.96302	838.48878	838.48878	559.32828	559.32828
$\beta 2i$	TTIAGLVFR	1700.98990	1700.98990	851.50223	851.50223	568.00391	568.00391
$\beta 5$	TTTLAFK	1504.85749	1504.85749	753.43602	753.43602	502.64644	502.64644
$\beta 5i$	TTTLAFK	1504.85749	1504.85749	753.43602	753.43602	502.64644	502.64644
$\beta 5t$	TTTLAFR	1532.86364	1532.86364	767.43909	767.43909	511.96182	511.96182

Table S2: Calculated exact (m/z) masses of the active-site peptides bound to biotin-epoxomicin (probe **3**).

The mono-isotopic mass (mono-iso) and the mass of the most abundant isotope peak (High-peak) are shown at charge (z) of 0, 2, and 3. The active site peptide sequence of $\beta 5$ and $\beta 5i$ is identical.

